ORIGINAL ARTICLE

Green synthesis of nanostructured silver particles and their catalytic application in dye degradation

CrossMark

Kumari Jyoti, Ajeet Singh *

Department of Biotechnology, Govind Ballabh Pant Engineering College, Pauri Garhwal, Uttarakhand 246194, India

Abstract Today, discharge of hazardous dyes from textile industries in water bodies like lakes, rivers and groundwater has become a serious problem, which contributes to increase their pollution levels significantly. These pollutants are difficult to remove by traditional water treatment procedures. Thus, there is a need to develop more suitable methods of effluent treatment. Here, we describe use of green-synthesized nanostructured silver particles in degradation of hazardous dyes like Safranine O, Methyl red, Methyl orange and Methylene blue etc. The silver nanoparticles (AgNPs) used as nanocatalysts were synthesized using *Zanthoxylum armatum* leaves. The reduction of silver ions and the formation of AgNPs have been assessed by UV–Vis spectroscopy. DLS, SEM–EDX, TEM, SAED and XRD studies revealed that the AgNPs were crystalline in nature with size range from 15 to 50 nm. The report emphasizes that the AgNPs are observed to be an excellent catalyst on reduction of hazardous dyes, which is confirmed by a decrease in absorbance maximum values.

1. Introduction

Recent advances in the field of nanotechnology and greater applications of nanoparticles have led to learn about the unexploited resources that already exist in nature for development of new methods in synthesis of nanoparticles. Generally, nanoparticles can be readily produced using physical and chemical methods [1]. However, these methods cannot avoid the generation of toxic byproducts in the synthesis protocol. Instead of using physical and chemical methods for synthesis

of metal nanoparticles, the use of biological resources available in nature including microorganisms [12] and plants [11] has received considerable attention for efficient and rapid synthesis of metal nanoparticles [22]. All the green methods are expected to minimize things that contribute to environmental problems and extremely offering a cost effective, eco-benign and energy efficient green alternative.

Foregoing facts revealed that the synthesis of metal nanoparticles by green chemistry approach is an exciting possibility that is relatively underexploited, which aroused our interest in the present investigation. The focus of the present work is to apply green chemistry approaches in the synthesis of silver nanoparticles (AgNPs) using aqueous leaf extracts of *Zanthoxylum armatum* as reducing and capping agents. *Z. armatum* is a perennial shrub belonging to the family Rutaceae

* Corresponding author. Mobile: +91 9997178236.
E-mail addresses: jyoti490sharma@gmail.com (K. Jyoti), ajeetsoniyal
@gmail.com (A. Singh).

and commonly known as toothache tree. The bark, fruits, seeds and leaves are extensively used in indigenous system of medicine as a carminative, stomachic, anthelmintic and in the treatment of fever, indigestion and abdominal pain [4].

Dyes are a major class of synthetic organic compounds used in variety of applications [10]. One of the applications of dyes is in textile industries which consumes about ∼60% of total dye production for coloration of various fabrics. Moreover after the completion of their use nearly 15% of dyes are wasted. These dye compounds dissolve in water bodies with a concentration in between 10 and 200 milligram per liter results in significant water pollution worldwide [9,7,17]. Therefore, treatment of dye effluents from textile industries is a mandatory part of waste water treatment. The release of dye effluents in aquatic systems is major environmental concern because coloration not only decreases sunlight penetration and dissolved oxygen in water bodies, but also releases toxic compounds during chemical or biological reaction pathway that effects aquatic flora and fauna [17]. Reduction of these dye compounds using physical–chemical and biological processes is generally ineffective, time consuming and methodologically demanding in a high effluent concentration [24]. Among such process, reductive degradation of hazardous dyes with metal nanomaterials is a convenient degradation process because of their unique physiochemical and electronic properties which are not present in bulk materials [5,2]. Metal nanomaterials are versatile materials that can be used in applications such as environmental remediation, medical technology, energy, water treatment, and personal care products [2,14]. Gold and silver nanoparticles can act as good catalysts and hence catalyze many reduction reactions. The rate constant of the catalytic reaction is found to depend on the size of the nanoparticles. The silver nanoparticles synthesized here are used as such to investigate its size dependant catalytic potential in the reduction of hazardous dyes.

2. Material and methods

2.1. Plant and chemicals

Fresh *Z. armatum* leaves were collected from Govind Ballabh Pant Engineering College campus and the sample was authenticated with the help of plant taxonomist of Forest Research Institute, Dehradun, Uttarakhand, India. Silver nitrate (99.99%), Safranine O, Methyl red, Methyl orange and Methylene blue were purchased from Sigma–Aldrich, Delhi.

2.2. Aqueous Z. armatum leaves extract preparation

The fresh *Z. armatum* leaves extract was prepared by taking 20 g of thoroughly washed finely cut leaves along with 100 ml of Milli-Q water in a 250 ml Erlenmeyer flask. The cut leaves were then boiled at 40 °C for 15 min. The solution was filtered through Whatman filter paper No. 1 and stored at 4 °C for further experiment.

2.3. Phytosynthesis of silver nanoparticles

AgNPs synthesis was carried out by taking 5% of leaf extract and adding 95% of 10^{-3} M aqueous AgNO₃ solution at 40 °C.

The change in color from colorless to brownish indicated the formation of silver nanoparticles.

2.4. Characterization of silver nanoparticles

Ultraviolet–visible spectral analysis was performed for all samples and the absorption maxima were recorded at a wavelength of 300–700 nm using spectrophotometer UV–Vis 3000 + LABINDIA. Fourier Transform Infrared Spectroscopy (FTIR) was used to detect the possible functional groups of biomolecules present in the plant extract. The surface morphology of the green synthesized AgNPs was examined using scanning electron microscopy (SEM) on NOVA-450 instrument, whereas shape, size, crystallinity and chemical composition were examined by transmission electron microscopy (TEM), selected area electron diffraction (SAED), X-ray diffraction (XRD) and energy dispersive spectroscopy (EDS) measurements on Tecnai G^2 20 S-TWIN instrument. The particle size distribution and surface charge of AgNPs were determined using particle size analyzer (Zetasizer nano ZS, Malvern Instruments Ltd., U.K.) at 25 °C with 90° detection angle.

2.5. Catalytic experiments

The catalytic activity of green synthesized AgNPs was demonstrated by degrading hazardous dyes, Safranine O, Methyl red, Methyl orange and Methylene blue. In general, 10 mg of each dye was added to 1 L of distilled water and used as stock solution. After that, 1 mg of green synthesized AgNPs was added to 10 ml of each dye solution and mixed ultrasonically for 15 min. Thereafter 3 ml of each mixed solution was used to evaluate the catalytic degradation of dyes.

The progress of reactions was monitored using UV–visible spectrophotometer by measuring absorbance maxima of dyes at different time intervals viz.,0.5 h, 1 h, 2 h, 3 h, 5 h, 8 h 12 h 18 h and 24 h. A control set was maintained without AgNPs for each dye and measured for absorbance.
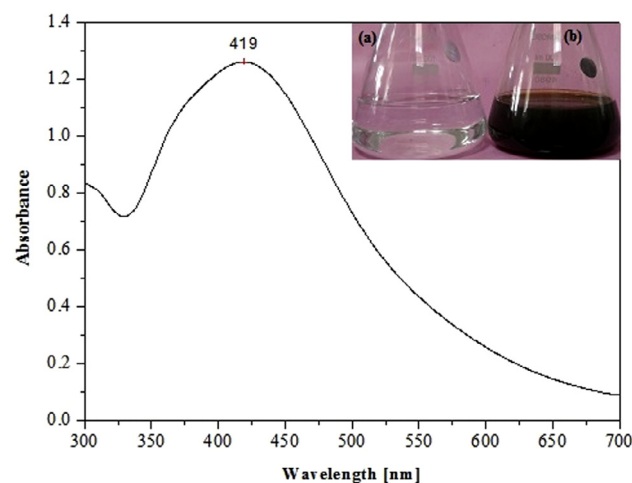

Figure 1 UV–visible spectra of synthesized silver nanoparticles. Insert: 1 mM AgNO₃ solution (a) without plant extract and (b) with plant extract.

3. Results and discussions

3.1. UV–visible absorption studies

The formation of silver nanoparticles was monitored on UV–visible spectrophotometer.

Surface plasmon resonance is a collective excitation of the electrons in the conduction band around the nanoparticles surface. Electrons conform to a particular vibration mode due to shape and size of particles. Therefore, metallic nanoparticles display characteristic optical absorption spectra in the UV–visible region [23]. Absorption spectra of silver nanoparticles showed a well defined surface Plasmon's band centered at around 419 nm. The appearance of brownish color observed is characteristic of excitation of surface plasmon vibrations which is absent in bulk material, while no color change was observed in absence of plant extract (Fig. 1 insert). This clearly indicates that the reducing agents present in extract of *Z. armatum* are involved in the reduction process.
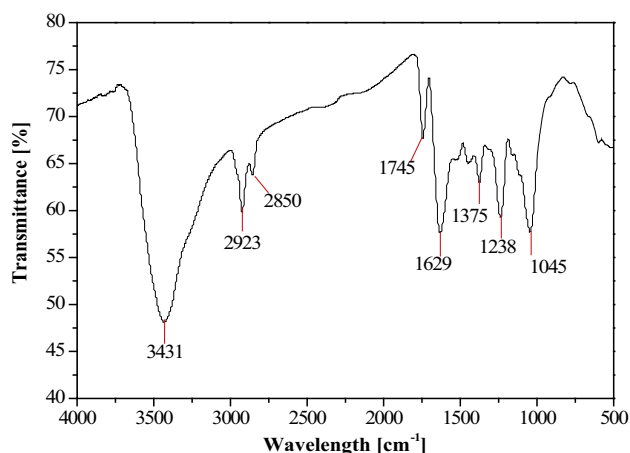

Figure 2 FTIR spectra of AgNPs synthesized by the reduction of AgNO$_3$ with the *Zanthoxylum armatum* leaf extract.

3.2. Fourier transforms infrared (FTIR) spectroscopy

In order to determine the functional groups in biomolecules of *Z. armatum* leaf extract and their role in the synthesis of AgNPs, FTIR analysis was done. Representative spectra of synthesized AgNPs (Fig. 2) manifests absorption peak located at about 3431, 2922, 1744, 1628, 1375, 1238 and 1045 in the region 500–4000 cm^{-1}.

The peak at 3431 cm^{-1} is associated with N—H stretching vibration of amino groups and indicative bond of —OH hydroxyl group suggesting the presence of phenols and a band at 2922 cm^{-1} is an indication of aliphatic C—H stretching. The peaks at1744 cm^{-1} are due to carbonyl stretching vibration of acid groups present in the extract. The peak at 1630 cm^{-1} is associated with N—H bond and is assigned to the amide I bonds of proteins [16]. In the present FTIR spectrum, there was also a peak at around 1628 cm^{-1}. The peaks at 1375 cm^{-1} and 1238 cm^{-1} are possibly the N=O symmetry stretching typical of the nitro compound of leaf extract and C—N-stretching of amines respectively. The peak at 1045 cm^{-1} corresponds to C—N (amines) stretch vibration of proteins. These results suggested that the biological molecules possibly perform dual function of synthesis and stabilization of silver nanoparticles [18]. It is well known that proteins can bind to AgNPs through free amine groups in the proteins [8] and therefore, stabilization of the AgNPs by surface-bound proteins.

3.3. Zeta sizer and Zeta potential

Zeta potential has been suggested to play an important role in the stability of nanoparticles. The zeta potential of green synthesized AgNPs was found to be −21.2 mV with average size ∼36 nm (Fig. 3a and b) suggesting that the surface of the nanoparticles was negatively charged that dispersed in the medium. The electrostatic repulsive forces between the nanoparticles upon negatively charged may prevent from aggregation which thereby increases the stability of the AgNPs [21].
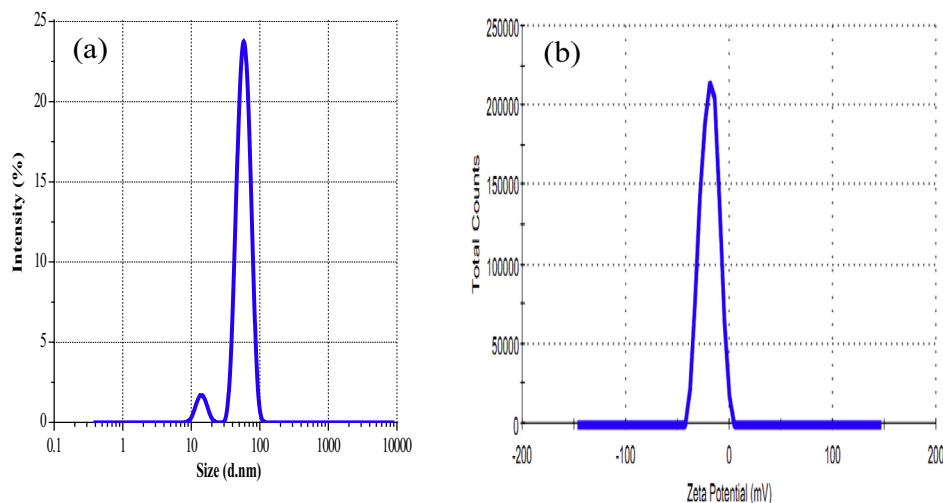

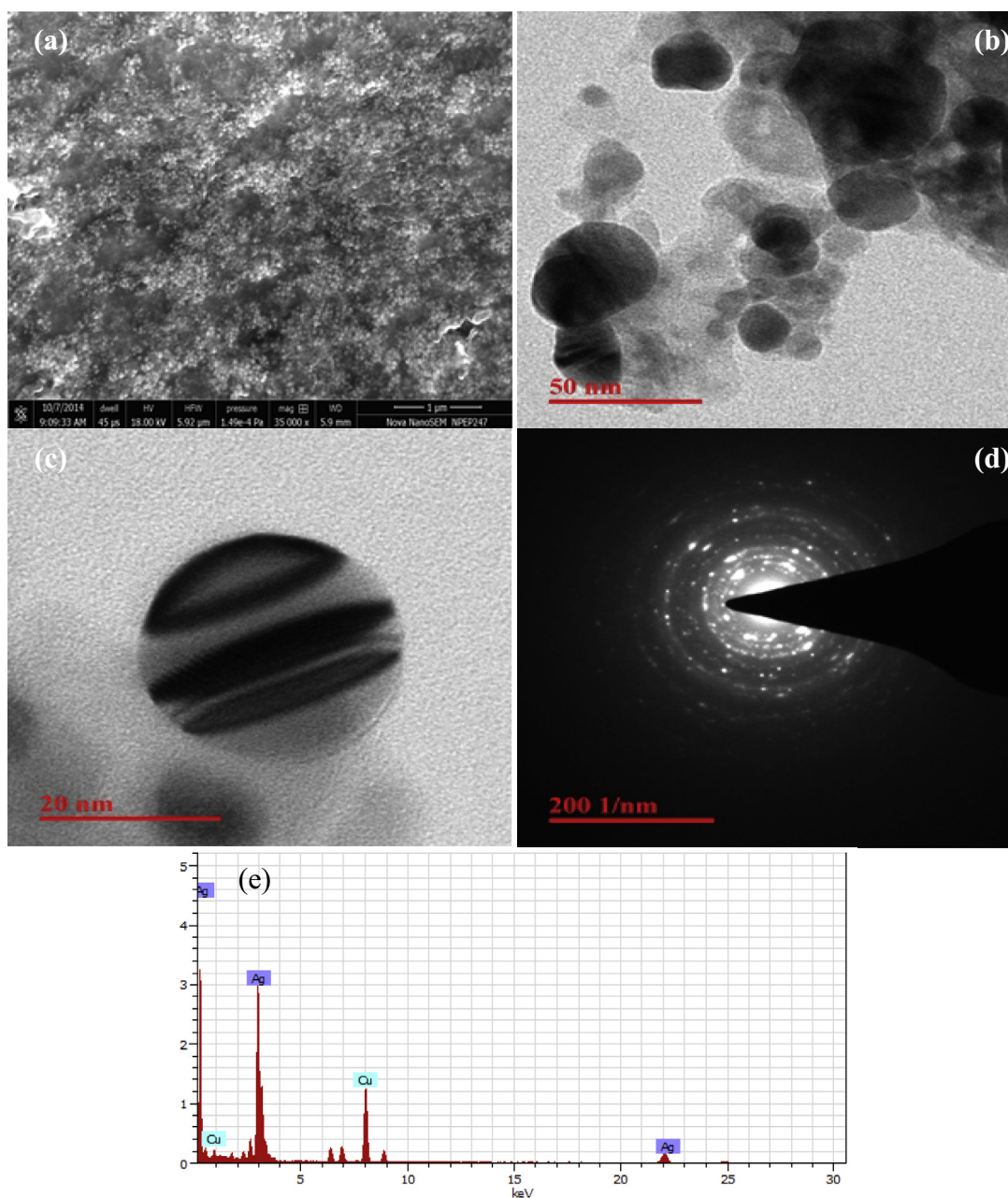**Figure 3** (a) Zeta sizer and (b) Zeta potential of green synthesized AgNPs.

Figure 4 (a) SEM image, (b) and (c) TEM images, (d) SAED image and (e) EDS of biosynthesized AgNPs from *Zanthoxylum armatum*.

3.4. SEM/TEM/SAED/EDS

Fig. 4(a) shows the SEM image of AgNPs on nanometric scale and it clearly indicated that the synthesized AgNPs are spherical in shape. TEM images of the formed AgNPs after termination of the reaction between the *Z. armatum* and AgNO₃ solution incubated at 40 °C for 10 min are presented in Fig. 4(b) and (c) that gives further insight into the particle size and size distribution.

From the Fig. 4(b), it is evident that the AgNPs were spherical in shape with a diameter of about 15–50 nm. The results obtained from the EDS give a clear indication regarding the elements of the nanoparticles. The strong signal of silver atom confirmed that silver nanoparticles contain pure silver

(Fig. 4e). The typical optical absorption between 2 and 4 KeV confirms the metallic nanoparticles due to surface plasmon resonance [13]. The other elemental signals of Cu in the EDS spectrum come from the TEM grid used. The silver particles were poly crystalline, and as could be seen from the selected area electron diffraction, all the AgNPs have single orientation forming a cluster of silver particles. Thus, synthesized AgNPs are highly crystalline as shown by clear lattice fringes and typical SAED (Fig. 4d).

3.5. X-ray diffraction (XRD)

A typical XRD pattern of AgNPs synthesized at 10 min of incubation period was found to possess face cubic centered
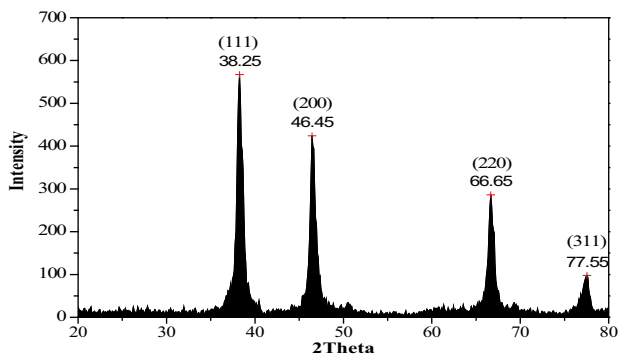
Figure 5 XRD pattern of phytosynthesized AgNPs prepared with *Zanthoxylum armatum* extract exhibiting the facets of crystalline silver.

structure. Fig. 5 shows the XRD pattern of the dried nanoparticles and suggests that the synthesized AgNPs are crystalline in nature.

The five broad diffraction peaks observed in the 2θ range at 20–$80° = 38.25, 46.45, 66.65$ and 77.55 can be indexed to the $(1 1 1)$, $(2 0 0)$, $(2 2 0)$ and $(3 1 1)$ orientations respectively, confirmed that the synthesized silver nanoparticles are composed of pure crystalline silver. The XRD patterns displayed here are consistent with earlier reports [19]. The average crystalline size is calculated using Debye–Scherrer formula,

$$D = \frac{k\lambda}{\beta \cos \theta}$$

where D is the average crystalline size of the nanoparticles, k is geometric factor (0.9), λ is the wavelength of X-ray radiation source and β is the angular FWHM (full-width at half maximum) of the XRD peak at the diffraction angle θ [3]. The calculated average crystalline size of the AgNPs is $\sim$22 nm.

3.6. Catalytic effects

3.6.1. Degradation of Safranine O

Safranine O is heterocyclic azine group of dyes, which is a derivative of phenazine. Presence of this dye in wastewater would have harmful effects on aquatic environment. The catalytic degradation of waste water containing Safranine O using AgNPs as catalysts was investigated. Fig. 6a represents that absorption band of Safranine O is known to appear at 519 nm. The degradation of safranine O was monitored by UV–visible spectrophotometer (Fig. 6a) and plot of $Ln(A/A_0)$ versus time for catalytic degradation of Safranine O is depicted in Fig. 6(b).

AgNPs are successfully used as a photocatalysts because of high surface to volume ratio, non toxic, cost effective and novel way of treatment of several dye pollutants. The results reveal that the rate of degradation of Safranine was visualized by a decrease in peak intensity within 24 h of incubation time.
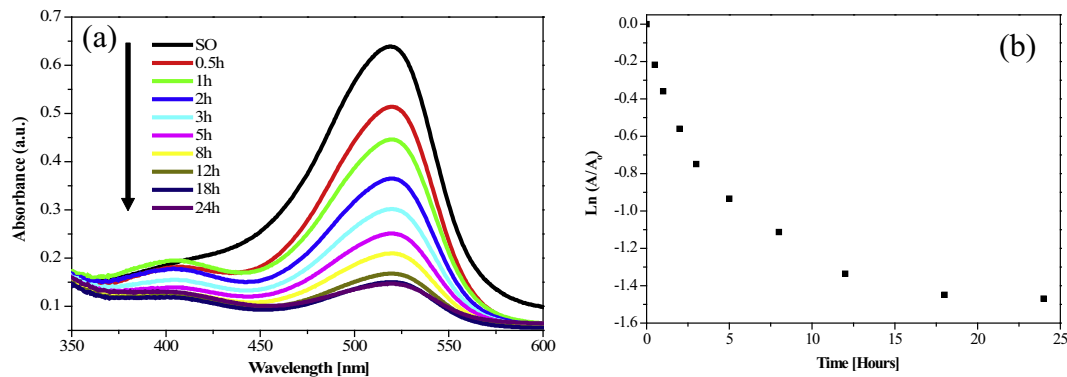

Figure 6 (a) UV–visible spectra of Safranine O reduction in the presence of synthesized AgNPs (b) Plot of $Ln(A/A_0)$ vs time (min) for catalytic degradation of Safranine O.
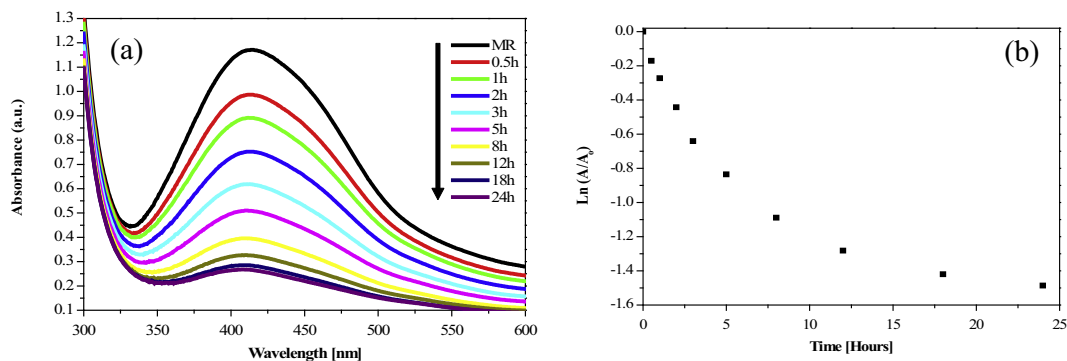

Figure 7 (a) UV–visible spectra of Methyl red reduction in the presence of synthesized AgNPs (b) Plot of $Ln(A/A_0)$ vs time for catalytic degradation of Methyl red.
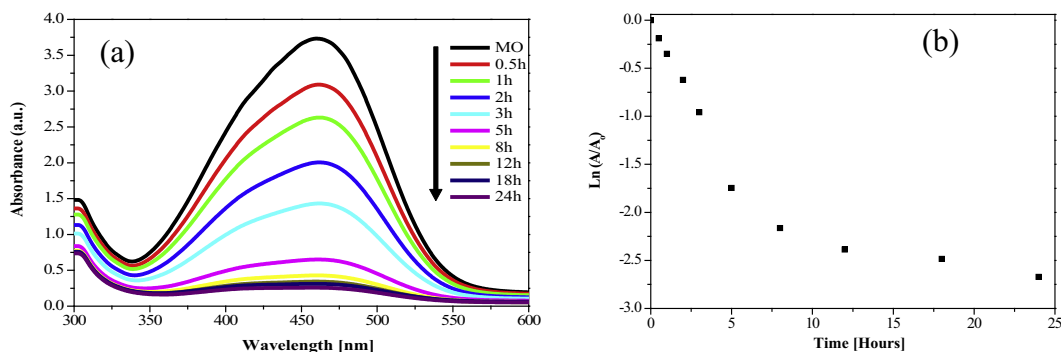
Figure 8 (a) UV–visible spectra of decomposition of methyl orange dye using AgNPs catalyst (b) Plot of $Ln(A/A_0)$ vs time for catalytic degradation of Methyl orange.
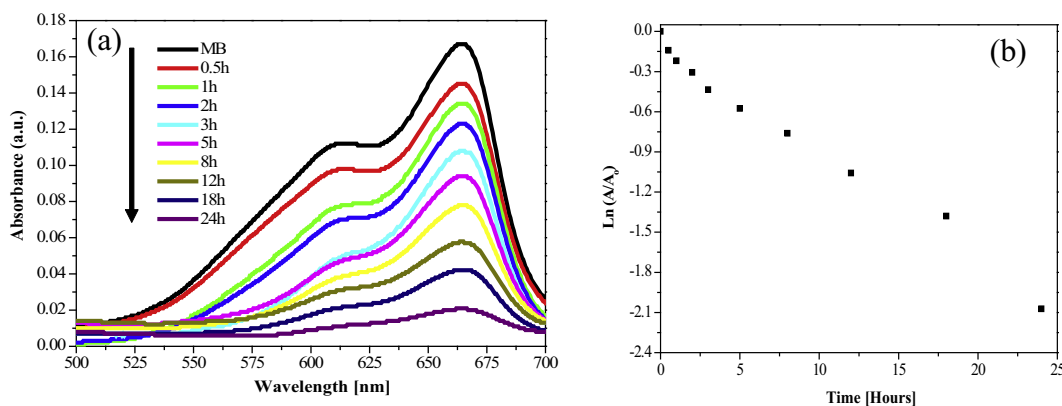

Figure 9 (a) UV–visible spectra of decomposition of Methylene blue dye using AgNPs catalyst (b) Plot of $Ln(A/A_0)$ vs time for catalytic degradation of methylene blue.

The calculated degradation rate constant value of Safranine O is 1.02×10^{-3} min^{-1}. The literature in catalysis research reveals that catalytic activity can be strongly dependant on the crystal structure, morphology and size of the particles [6].

3.6.2. Degradation of Methyl red

The release of dye effluents from textile industry is a major source of water pollution. Methyl red is one of pollutant of waste water and has potential threat to the environment, therefore, treatment of Methyl red is highly desirable. Fig. 7(a) shows the degradation of Methyl red in the presence of AgNPs as photocatalysts and plot of $Ln(A/A_0)$ vs time for catalytic degradation of Methyl red by AgNPs is shown in Fig. 7b. The degradation rate constant value of Methyl red is 1.03×10^{-3} min^{-1}. The main absorption peak at 415 nm decreased gradually with the extension of exposure time, indicating the catalytic degradation of Methyl red dye.

3.6.3. Degradation of Methyl orange

We studied the degradation of wastewater containing Methyl Orange (MO), a commonly used azo dye [15], using green synthesized AgNPs as catalysts. Fig. 8(a) represents that absorption band of MO is known to appear at 460 nm. It can be observed that after adding AgNPs to the MO, the absorption band of MO at 460 nm gradually disappears with varying time

intervals. The plot of relative absorption intensity with wavelength in a regular interval of time reveals that the degradation of MO occurs in 24 h in the presence of AgNPs catalysts. Plot of $Ln(A/A_0)$ vs time for catalytic degradation of Methyl orange by AgNPs is depicted in Fig. 8(b) and calculated degradation rate constant value of Methyl orange is 1.86×10^{-3} min^{-1}.

3.6.4. Degradation of Methylene blue

In order to investigate the catalytic activity of AgNPs, reduction of methylene blue (water contaminant) was carried using green synthesized AgNPs at varying time intervals in the visible region (Fig. 9a). Methylene blue is a heterocyclic aromatic chemical compound with molecular formula $C_{16}H_{18}C_1N_3S$. The extent of degradation of Methylene blue using AgNPs as catalyst was monitored by UV–visible spectroscopic technique. The absorption peaks for Methylene blue dye in water was found to be centered at 664 nm in the visible region [20]. In the presence of AgNPs as a catalyst, absorption spectrum showed the decreased peaks for Methylene blue with varying time intervals. The reduction of Methylene blue dye was evident from the gradual decrease of the absorbance value of dye approaching the baseline and increased peak for silver nanoparticles. Finally it disappeared with the increase of reaction time, which indicates that the degradation of Methylene blue dye occurs. Plot of $Ln(A/A_0)$ vs time for catalytic degra-

dation of Methylene blue by AgNPs is depicted in Fig. 9(b) and calculated degradation rate constant value of Methylene blue is 1.44×10^{-3} min^{-1}.

4. Conclusion

In this study, a simple and convenient method is developed for the preparation of silver nanoparticles. These synthesized silver nanoparticles were used as catalysts in the process of degradation of hazardous dyes in a cost effective manner. In the presence of silver nanoparticles as catalysts, the degradation efficiency is increased due to their very high surface area as well as accelerate migration rate of electrons/hole to the surface of the nanoparticles. Degradation efficiency is increased with varying time intervals and degradation process completed within 24 h. Therefore, it can be concluded that our study can provide a novel method for the controlled synthesis of size and shape dependent silver nanoparticles, which can widely be used in the treatment of dye effluent from industries. Moreover, this method for synthesis of silver nanoparticles offers efficient, economic and eco-friendly approach that does not need any special conditions such as vacuum conditions, catalysts and sophisticated instruments.

Acknowledgements

References

[1] A. Alqudami, S. Annapoorni, Plasmonics 2 (2007) 5–13.
[2] M.H.N. Amini, S.M.F. Farnia, New J. Chem. 38 (2014) 1581–1586.
[3] V. Balaji, S. Vimala, T. Anusha, V. Elangovan, Asian Pac. J. Trop. Dis. 7 (2014) 294–300.
[4] M.I. Barkatullah, N. Muhammad, Afr. J. Pharm. Pharmacol. 5 (2011) 1718–1723.
[5] S. Caudo, G. Centi, C. Genovese, S. Perathoner, Top. Catal. 40 (2006) 207–209.
[6] J. Das, P. Velusamy, J. Taiwan Inst. Chem. E 45 (2014) 2280–2285.
[7] A.K. Dutta, S.K. Maji, B. Adhikary, Mater. Res. Bull. 49 (2013) 28–34.
[8] A. Gole, C. Dash, V. Ramachandran, A.B. Mandale, S.R. Sainkar, M. Rao, M. Sastry, Langmuir 17 (2001) 1674–1679.
[9] K.H. Gonawala, M.J. Mehta, J. Eng. Res. Appl. 4 (2014) 102–109.
[10] M.H. Habibi, E. Askari, Iran. J. Catal. 1 (2011) 41–44.
[11] K. Jyoti, M. Baunthiyal, A. Singh, J. Radiat. Res. Appl. Sci. 9 (2016) 217–227.
[12] Y. Konishi, K. Ohno, N. Saitoh, T. Nomura, S. Nagamine, H. Hishida, Y. Takahashi, T. Uruga, J. Biotechnol. 128 (2007) 648–653.
[13] P. Magudapatty, P. Gangopadhyayrans, B.K. Panigrahi, K.G. M. Nair, S. Dhara, Phys. B 299 (2001) 142–146.
[14] M.M. Najafpour, F. Rahimi, M. Amini, S. Nayeri, M. Bagherzadeh, Dalton Trans. 41 (2012) 11026–11031.
[15] T. Panakoulias, P. Kalatzis, D. Kalderis, A. Katsaounis, J. Appl. Electrochem. 40 (2010) 1759–1765.
[16] P. Prakash, P. Gnanaprakasam, R. Emmanuel, S. Arokiyaraj, M. Saravanan, Colloids Surf. B 108 (2013) 255–259.
[17] A. Predescu, A. Nicolae, U.P.B. Sci, Bull. Ser. B 74 (2012) 1454–2331.
[18] R. Sathyavathi, M.B. Krishna, S.V. Rao, R. Saritha, D.N. Rao, Adv. Sci. Lett. 3 (2010) 1–6.
[19] M. Satishkumar, K. Sneha, S.W. Won, C.W. Cho, S. Kim, Y.S. Yun, Colloids Surf. B 73 (2009) 332–338.
[20] T. Shahwan, S. Abu Sirriah, M. Nairat, E. Boyacı, A.E. Eroglu, T.B. Scott, K.R. Hallman, Chem. Eng. J. 172 (2011) 258–266.
[21] A.K. Suresh, M.J. Doktycz, W. Wang, J.W. Moon, B. Gu, H.M. Meyer, D.K. Hensley, D.P. Allison, T.P. Phelps, D.A. Pelletier, Acta Biomater. 7 (2011) 4253–4258.
[22] K.P. Upendra, S.S. Preeti, S. Anchal, Dig. J. Nanomater. Biostruct. 4 (2009) 159–166.
[23] G. Wang, S. Chunsheng, Z. Naiqin, D. Xiwen, Mater. Lett. 61 (2007) 3795–3797.
[24] D. Wesenberg, I. Kyriakides, S.N. Agathos, Biotechnol. Adv. 22 (2003) 161–187.